Manuscript Click here to view linked References

A Multi-Star Synchronous Machine Model for Real-Time Digital Simulation and Its Applications

A. B. Dehkordi and T. L. Maguire

***Abstract*— Poly-phase electric machines have the advantages of low ripple in torque, better fault tolerance and high reliability in operation. Such properties make them attractive for applications in renewable energies, electric ship propulsion, traction, aircraft systems and electric vehicles [1]-[2]. Failure of the drive system through a few phases could be tolerated by operating the remaining phases of the machine. One popular group amongst poly-phase electric machines is the category of multi-star machines.**

This paper presents development and validation of a multi-star synchronous machine model for a real-time digital simulator. The paper starts with the introduction and analysis of multi-star machines. A generalized method of Vector-Space Decomposition (VSD) is introduced for analyzing machines with an arbitrary number of stars. The method of incorporating the model into the network solution of real-time electromagnetic transient program is described. For the purpose of demonstration, a typical circuit of a marine electric vessel, containing poly-phase generators, power electronic converters, DC bus, hotel load, battery, and poly-phase propulsion systems is simulated in real time.

***Keywords*: poly-phase, multi-star synchronous machine, symmetrical components, VSD, two reaction theory, real-time digital simulation, digital transient network analyzer, wind generation, electric ship.**

I. Introduction

In conventional power system applications, the number of phases is three as it generally results in a lower transmission costs. Historically 3-phase systems are selected for transmission and electric machines in both generation and loads. When it comes to applications where the electric machine is connected to power electronic converters, restriction to a system with 3 phases is not necessary [1].

Historically, electric machines with higher number of phases (poly-phase machines) were introduced to lower the ripples in electric torque, and to lower current ratings per phase. In fact, the later was a reason that promoted the development of multi-phase machines in early stages of circuit breaker development. Additionally, lower current rating per phase allows the deployment of power electronic converters with lower ratings.

In addition to lower torque ripple and current ratings, poly-phase machines have other advantages such as higher force density, reduction in the noise characteristic and the stator copper losses [2]. Additionally, poly-phase machines have greater reliability and fault tolerance. Several phases can be lost yet the machine can still be operated utilizing the remaining phases by providing proper excitation through power electronic converters.

For the above reasons, poly-phase machines have applications in electric ship propulsion, traction, aircraft systems, electric vehicles [2]-[3] and new schemes of wind turbines. There are variations of poly-phase machines such as split-phase, multi-star, higher order symmetrical, etc., which can be studied in literature [2]-[3].

A real time digital simulator is a combination of computer hardware and software designed specifically for the solution of power system and power electronic electromagnetic transients in real time. There are many areas where this technology has been successfully applied. Simulation of electric networks in marine vessels is one of such applications. Modeling of poly-phase machines for real-time digital simulation is an important step in enhancing these simulators for marine applications.

Modeling of poly-phase machines poses several challenges, especially when it comes to real-time digital simulation. One of the main problems is the diversity of these models; even if the phases are displaced in a symmetric manner, the number of phases may vary between 3 to 18 or even more [4]. Developing and maintaining a large number of machine models in the library of any commercial software is challenging and time-consuming.

A comprehensive analysis in rotor frame of reference is necessary as it responds to the question of general analysis of poly-phase machines. Note that, in practical applications, these machines are driven by power electronic converters with high frequency switching; therefore, models need to be implemented with a smaller simulation time-step of a few microseconds. This makes the modeling in rotor frame of reference more attractive.

As mentioned earlier, there are various types of poly-phase machines models; two main categories are symmetrical multi-phase machines and multiple-star machines. In symmetrical multiphase machines, N stator phases are distributed symmetrically in the stator space with the angular displacement of $2\pi/N$. In multiple-star machines, stator is made of l winding sets (stars) with k phases for each winding set. Naturally, number of phases is of $k.l$. In multiple star machines, the angular displacement between winding sets is commonly designed to be π/N. There are other types of multi-star machine where the angular displacement between winding sets is arbitrary. Modeling of such machines is not in the focus of this paper.

This paper presents the development of a multi-star synchronous machine model for real-time digital simulation. The paper starts with the introduction and analysis of multi-star synchronous machines. Differential equations of a multi-star synchronous machine are described and challenges of

A. B. Dehkordi is with RTDS Technologies Inc., Winnipeg, Canada (e-mail: dehkordi@rtds.com).
T. L. Maguire is with RTDS Technologies Inc., Winnipeg, Canada (e-mail: dehkordi@rtds.com).

Paper submitted to the International Conference on Power Systems Transients (IPST2021) in Belo Horizonte, Brasil June 6-10, 2021.

modeling and analysis in these machines are outlined.

The so-called method of Vector Space Decomposition (VSD) is proposed for extending the two-reaction theory [5]-[6] to multi-star arrangements [7]-[10]. A general equivalent circuit in rotor frame of reference is presented from which a transient multi-star synchronous machine model is developed and incorporated into the network solution of a real-time digital simulator. Capabilities of the model such as flexibility in selecting the number of stars are described. Additionally, the method of simulating power electronic converters based on a predictive switching algorithm is introduced. To demonstrate the capabilities of the model, a typical circuit of marine electric vessel, containing poly-phase generators, power electronic converters, DC bus, hotel load, battery, and poly-phase propulsion systems is simulated in real time with a time-step of 3 µs, and the results are shown.

II. Analysis of Multi-Star Synchronous Machines

This section briefly describes the analysis and modeling method of multi-star synchronous machines. Since the goal is incorporation of the model into an electromagnetic transient program [11], the coupled electric circuit approach is used for modeling of this type of machine. The machine is considered as an idealized machine assuming sinusoidal distribution for the magneto-motive forces and permeance.

A. General Description of a Multi-Star Synchronous Machine

As described, in a multiple-star machine, stator is made of *l* winding sets (stars) with *k* phases for each winding set. Naturally, number of phases is $N = l.k$. In such machines, the angular displacement between winding sets is commonly designed to be π/N. As an example, an idealized winding diagrams for a 6-phase multi-star (dual-star) machine is shown in Fig. 1. The diagram shows the axis of each winding, which is defined as the axis of MMF produced by that winding.

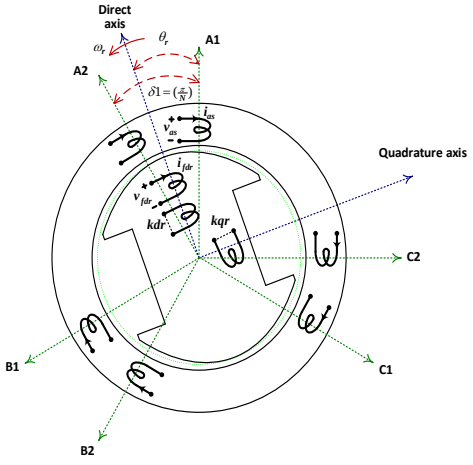

Fig. 1. Idealized winding configuration for a multi star 6-phase synchronous machine.

B. Multi-Star Winding Configuration and Transformation to Fundamental Winding Configuration

Consider the simplified arrangement of a symmetrical poly-phase stator. Several sets of coils distributed symmetrically around the periphery of the two-pole stator covering *360°*. This is generally called *two-pole symmetry*. The *fundamental* winding arrangement with *180°* progression (shown in Fig. 2.) is referred to as *single-pole symmetry*, or more simply, *pole-symmetry* [9]. From design point of view, such a winding arrangement works as well as the full progression winding arrangement. In fact, a single-phase induction machine, which is a two-phase machine with *90°* angular shift between the winding sets, has a pole-symmetry.

It is shown in [7]-[9] that a multi-star arrangement can be transformed to a symmetrically distributed winding arrangement with *180°* progression called fundamental winding configuration. Fig. 2 shows the fundamental winding arrangement for a 6-phase machine. The purpose of this diagram is to show the axes of windings in this arrangement. As can be seen in this figure, six windings are distributed with a spatial angular shift of $\delta 1 = 180°/6 = 30°$, and a total progression of *180°*.

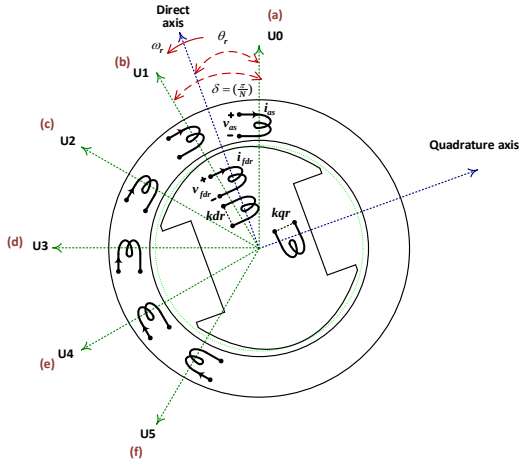

Fig. 2. Idealized winding configuration for a fundamental arrangement 6-phase synchronous machine.

Variables in multi-star configurations such as voltages, currents and flux linkages can be easily transformed into corresponding variables in fundamental winding arrangement [7] and [9]. As an example, for a dual-star 6-phase machine (*k=3, l=2*), the relation between the multi-star variables and fundamental winding variables are shown in (1).

$$(f_a\ f_b\ f_c\ f_d\ f_e\ \ f_f)^T = W_{2\times 3}\cdot(f_{A1}\ f_{B1}\ f_{C1}\ f_{A2}\ f_{B2}\ \ f_{C2})^T \quad (1)$$

where:

$$[W_{2\times 3}] = \begin{bmatrix} 1 & 0 & 0 & 0 & 0 & 0 \\ 0 & 0 & 0 & 1 & 0 & 0 \\ 0 & 0 & -1 & 0 & 0 & 0 \\ 0 & 0 & 0 & 0 & 0 & -1 \\ 0 & 1 & 0 & 0 & 0 & 0 \\ 0 & 0 & 0 & 0 & 1 & 0 \end{bmatrix}$$

C. Voltage and Flux Linkage Equations

Based on the above description of a multiple-star synchronous machine, voltage and flux linkage equations are developed. The following assumptions are made in this analysis:

- A multi-pole synchronous machine is modeled as an equivalent two-pole machine.
- It is assumed that the machine windings produce a sinusoidal MMF, and permeance is sinusoidally distributed; therefore, space harmonics are ignored. Basically, the machine is assumed an idealized machine.
- Although the magnetizing MMF is assumed sinusoidal, effects of space harmonics in cross-coupling leakage between stator winding, (i.e. differential leakage) is

considered. That means that, the leakage inductance matrix of stator may have off-diagonal elements that are taken into consideration.

- By definition, stator is made of *l* winding sets (stars) with *k* phases for each winding set. Number of phases is $N = l.k$, and the angular displacement between winding sets is π/N. Phase resistances are equal, and leakage inductances are symmetrical with respect to each winding.

Voltage and flux linkage equations for a N-phase multi-star synchronous machine are presented in (2). Equation (2) shows the relation between vectors of voltages, currents and flux linkages of the machine. Here, vectors of stator voltages, currents and flux linkages are by $\underline{v}_{A1B1\ldots Kl_s}$, $\underline{i}_{A1B1\ldots Kl_s}$ and $\underline{\psi}_{A1B1\ldots Kl_s}$ respectively. A similar arrangement is made for rotor quantities.

$$\begin{pmatrix} \underline{v}_{A1B1\ldots Kl_s} \\ \underline{v}_{dq_r} \end{pmatrix} = \begin{pmatrix} [r_s] & [0] \\ [0] & [r_s] \end{pmatrix} \begin{pmatrix} \underline{i}_{A1B1\ldots Kl_s} \\ \underline{i}_{dq_r} \end{pmatrix} + \frac{d}{dt} \begin{pmatrix} \underline{\psi}_{A1B1\ldots Kl_s} \\ \underline{\psi}_{dq_r} \end{pmatrix}$$

$$\begin{pmatrix} \underline{\psi}_{A1B1\ldots Kl_s} \\ \underline{\psi}_{dq_r} \end{pmatrix} = \begin{pmatrix} [L_{ss}] & [L_{sr}] \\ [L_{sr}]^T & [L_{rr}] \end{pmatrix} \begin{pmatrix} \underline{i}_{A1B1\ldots Kl_s} \\ \underline{i}_{dq_r} \end{pmatrix} \quad (2)$$

where:

$$(\underline{f}_{A1B1\ldots A2B2\ldots AlBl\ldots_s})^T = (f_{A1}\, f_{B1} \cdots f_{A2}\, f_{B2}\, \ldots\ldots\, f_{Al}\, f_{Bl}\, \ldots)$$

$$(\underline{f}_{dq_r})^T = (f_{dr_1}\, f_{dr_2} \cdots f_{qr_1}\, f_{qr_2}\, \ldots)$$

When the number of phases per set is 3 (i.e. *k=3*), the well-known 3-phase Park transformation with suitable angular shifts may be used to transform the phase domain equations of (2) into rotor frame of reference [12] and [13]. One of the drawbacks of this method is that due to Toeplitz structure of the leakage inductance matrix, cross-coupling terms may appear between the d- and q- equivalent circuits [7] and [12]. Furthermore, the method is not applicable if the number of phases per set is not 3 ($k \neq 3$).

A more general approach used here, is the so-called vector space decomposition (VSD). The basis of this approach is the fact that symmetrical component transformation introduced by Fortescue [14] is applicable to systems with any number of phases. It is also well known that, this transformation diagonalizes circulant (cyclic symmetric) matrices [15]-[16]. One can prove that, due to symmetry, the inductance matrix of a symmetrical poly phase machine with 360° phase progression is cyclic symmetric. Therefore, symmetrical component transformation diagonalizes the stator inductance matrix of a symmetrical poly phase machine with any number of phases. Ku and White extracted αβ and dq transformations based on this property for any number of phases [15]. These transformations also diagonalize the inductance matrix of symmetrical poly-phase machines.

For multiple star machines, a similar approach can be adapted. It is shown in the previous section that, any multi-star winding arrangement can be transformed to a fundamental winding arrangement with 180° phase progression [7]-[9]. Based on the analogy in the previous paragraph, a new symmetrical component transformation for windings with 180° phase progression can be developed, and consequently, *αβ* and *dq* transformations can be established [7] and [9]. These transformations diagonalize the inductance matrix of machines with 180° phase progression windings. As an example, for a dual-star 6-phase machine (k=3, l=2), the general two-phase (*αβ*) transformation from fundamental winding variables to *αβ* components are shown in (3). In this transformation, the first and the last row correspond to the fundamental *αβ* components. Other rows correspond to harmonic components. In the absence of winding spatial harmonics, these components do not produce a revolving field; therefore, they can be considered zero sequences. Note that, if the number of phases is odd, there will be a row in this transformation corresponding to the homo-polar zero sequence.

$$(f_{\alpha 1}\, f_{\alpha 3}\, f_{\alpha 5}\, f_{\beta 5}\, f_{\beta 3}\; f_{\beta 1})^T = C_\alpha^a \cdot (f_a\, f_b\, f_c\, f_d\, f_e\; f_f)^T$$

where:

$$\left[C_\alpha^a\right] = \left(\frac{2}{N}\right) \cdot \begin{bmatrix} 1 & \cos(\delta 1) & \cos(2\delta 1) & \cos(3\delta 1) & \cos(4\delta 1) & \cos(5\delta 1) \\ 1 & \cos(3\delta 1) & \cos(6\delta 1) & \cos(9\delta 1) & \cos(12\delta 1) & \cos(15\delta 1) \\ 1 & \cos(5\delta 1) & \cos(10\delta 1) & \cos(15\delta 1) & \cos(20\delta 1) & \cos(25\delta 1) \\ 0 & \sin(5\delta 1) & \sin(10\delta 1) & \sin(15\delta 1) & \sin(20\delta 1) & \sin(25\delta 1) \\ 0 & \sin(3\delta 1) & \sin(6\delta 1) & \sin(9\delta 1) & \sin(12\delta 1) & \sin(15\delta 1) \\ 0 & \sin(\delta 1) & \sin(2\delta 1) & \sin(3\delta 1) & \sin(4\delta 1) & \sin(5\delta 1) \end{bmatrix} \quad (3)$$

$$\delta 1 = \frac{\pi}{6}$$

Based on the above, the following methodology is used to analyze multi-star machines: first transform the variables to fundamental winding variables, then use *αβ* or *dq* transformations to decouple the equations. After solving the equations in the decoupled form (rotor frame of reference), transform them back to fundamental winding quantities and then eventually obtain all multi-star quantities.

Voltage and flux linkage equations for an N-phase synchronous machine with 180° phase progression are presented in (4). Here, vectors of stator voltages, currents and flux linkages are shown by $\underline{v}_{ab\ldots n_s}$, $\underline{i}_{ab\ldots n_s}$ and $\underline{\psi}_{ab\ldots n_s}$ respectively. Self-inductance matrices of stator and rotor are shown by $[L_{ss}]$ and $[L_{rr}]$. $[L_{sr}]$ is the matrix for the mutual inductances between the stator and rotor windings. The values of these inductances are functions of rotor position θ_r and saturation. As an example, the stator inductance matrix $[L_{ss}]$ is shown in (5). Inductance values M_{0s} and L_{2s} are functions of winding distribution, effective number of turns, effective air-gap length and saturation. As mentioned previously, higher order space harmonics of the machine are ignored.

$$\begin{pmatrix} \underline{v}_{ab\ldots n_s} \\ \underline{v}_{dq_r} \end{pmatrix} = \begin{pmatrix} [r_s] & [0] \\ [0] & [r_s] \end{pmatrix} \begin{pmatrix} \underline{i}_{ab\ldots n_s} \\ \underline{i}_{dq_r} \end{pmatrix} + \frac{d}{dt} \begin{pmatrix} \underline{\psi}_{ab\ldots n_s} \\ \underline{\psi}_{dq_r} \end{pmatrix}$$

$$\begin{pmatrix} \underline{\psi}_{ab\ldots n_s} \\ \underline{\psi}_{dq_r} \end{pmatrix} = \begin{pmatrix} [L_{ss}] & [L_{sr}] \\ [L_{sr}]^T & [L_{rr}] \end{pmatrix} \begin{pmatrix} \underline{i}_{ab\ldots n_s} \\ \underline{i}_{dq_r} \end{pmatrix} \quad (4)$$

where:

$$(\underline{f}_{ab\ldots n_s})^T = (f_{as}\, f_{bs} \cdots f_{ns})$$

$$(\underline{f}_{dq_r})^T = (f_{dr_1}\, f_{dr_2} \ldots f_{qr_1}\, f_{qr_2}\, \ldots)$$

Leakage Inductance Matrix:

The leakage inductance matrix of the stator is shown by $[L_{ss\text{-}l}]$. In symmetrical multi-phase machines, this matrix usually has a circulant (cyclic symmetric) structure whereas for windings with single-pole symmetry, it has a Toeplitz structure [7]. The existence of non-zero off-diagonal elements may come as a surprise to some; although the magnetizing MMF is assumed sinusoidal, effects of space harmonics in cross-coupling leakage between stator winding, (i.e. differential leakage) is considered. This causes the leakage inductance matrix to have off-diagonal elements [7]. The leakage values l_0, l_1 and so on in (6) are functions of winding

distributions and dimensions.

Application of symmetrical component or αβ transformations with 180° phase progression diagonalizes this Toeplitz-structured leakage inductance matrix [7]. This is demonstrated in (7). Note that, if the off-diagonal elements of the leakage inductance matrix are not available, or if these elements are not intended for consideration, then users may consider a diagonal leakage inductance matrix. The elements of this diagonal matrix are all equal to the stator self-leakage.

$$\left[L_{ss}\right]=\left[L_{ss-l}\right]+\left[L_{ss-oh}\right]+\left[L_{ss-2h}\right]$$

where:

$$\begin{cases}\left[L_{ss-0h}\right]_{ik}=(\frac{2}{N})\cdot M_{0s}\cdot\cos\left[(k-i)\delta\right]\\ \left[L_{ss-2h}\right]_{ik}=(\frac{2}{N})\cdot L_{2s}\cdot\cos\left[2\theta_r-(i+k-2)\delta\right]\end{cases}\quad(5)$$

$$\delta=(\tfrac{2\pi}{N})\quad i,k\in 1,2\ldots N$$

$$\left[L_{ss-l}\right]=\begin{bmatrix} l_0 & l_1 & l_2 & \cdots & -l_3 & -l_2 & -l_1\\ l_1 & l_0 & l_1 & \cdots & -l_4 & -l_3 & -l_2\\ l_2 & l_1 & l_0 & \cdots & -l_5 & -l_4 & -l_3\\ \cdots & \cdots & \cdots & & \cdots & \cdots & \cdots\\ -l_3 & -l_4 & -l_5 & \cdots & l_0 & l_1 & l_2\\ -l_2 & -l_3 & -l_4 & \cdots & l_1 & l_0 & l_1\\ -l_1 & -l_2 & -l_3 & \cdots & l_2 & l_1 & l_0\end{bmatrix}\quad(6)$$

$$\left[L_{ss-l}\right]^{dq}=\begin{bmatrix} L_{ls-h1} & 0 & 0 & \cdots & 0 & 0 & 0\\ 0 & L_{ls-h3} & 0 & \cdots & 0 & 0 & 0\\ 0 & 0 & L_{ls-h5} & \cdots & 0 & 0 & 0\\ \cdots & \cdots & \cdots & L_{ls-hm} & \cdots & \cdots & \cdots\\ 0 & 0 & 0 & \cdots & L_{ls-h5} & 0 & 0\\ 0 & 0 & 0 & \cdots & 0 & L_{ls-h3} & 0\\ 0 & 0 & 0 & \cdots & 0 & 0 & L_{ls-h1}\end{bmatrix}\quad(7)$$

$$L_{ls-hm}=l_0+2\cdot\sum_{k=1}^{truc(\frac{N-1}{2})}l_k\cdot\cos(m\cdot k\cdot\delta 1)$$

D. Equivalent Circuit in DQ frame of Reference

The DQ Equivalent circuit of an N-phase synchronous machine with 180° phase progression is shown in Fig. 3. This circuit is effectively applicable to a multi-star synchronous machine as well. Note that, in addition to the d- and q- axis equivalent circuits, there exist other equivalent circuits corresponding to harmonics (3, 5, ...). In an idealized machine with perfectly sinusoidally wound stator, these harmonics do not produce a revolving field. In this case, these circuits are effectively zero-sequence circuits, as they do not couple with the rotor. Note that if the number of phases is odd, there will also exist a homo-polar zero sequence circuit. Leakage inductance values *Lls-h1*, *Lls-h3*, and *Lls-h5* are the leakage inductances corresponding to each harmonic. These values are the diagonal elements of the leakage matrix after the application of *αβ* transformation. Note that, the model introduced in this paper receives these values as input, and prints the full phase-domain leakage matrix of the stator in a separate file for the users.

It is shown that, in multi-phase machines *N>3*, the method of VSD can make a position-independent inductance matrix in dq frame of reference, even in the presence of some of the space harmonics [1], [7] and [17]. In this case, these harmonics contribute to the revolving field, thus the harmonic equivalent circuits in Fig. 3 need to be modified to account for the coupling of stator and rotor circuit. In the model presented here, these effects are ignored, since such data is not available to most users.

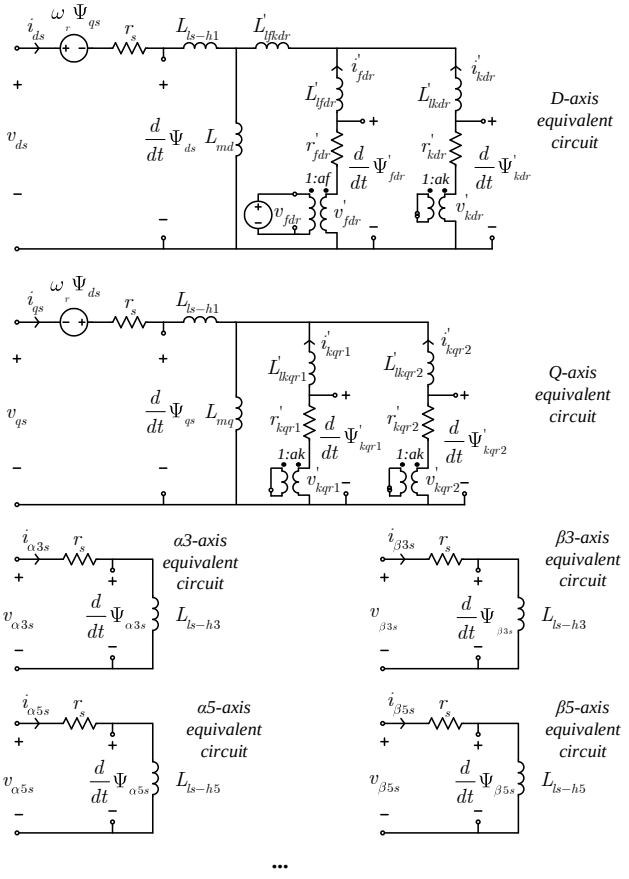

Fig. 3. Equivalent circuit of an idealized N-phase synchronous machine with 180° phase progression.

III. Implementation of the Multi-Star Synchronous Machine Model into the Environment of the Real-Time Digital Simulator

Each unit of the real-time digital simulator used in this paper, consists of processors or cores dedicated to the solution of the power system networks, power system devices, and control components [18]. Each simulation time-step is divided into computation intervals and communication intervals. Similar to other electromagnetic transient programs such as EMTP and EMTDC, Dommel algorithm [11] is used for discretization of the electric system's differential equation. In this method, passive RLC elements of the circuit, as well as, more sophisticated components such as, machines, transformers and power electronics are represented by companion circuits in the form of current sources and conductances [11]. Subsequently, the nodal solution is used for calculation of node voltages. Due to the fact that, multi-phase machines are usually connected to power electronic converters with high frequency switching, usually a small simulation time-step of a few microseconds needs to be used to model systems containing such machines.

<u>Features and Capabilities of the Model:</u>

This section describes the capabilities of the model proposed here. The modeling technique can be applied to any number of stars and any number of phases per star. The current implemented model, however, only considers 3-phase stars. The number of stars for the machine can be selected by the user from a menu. Based on the selected number of phases, stator terminals and neutral will be available for external

connection. Additionally, an option is available to access both ends of each stator winding. This option allows users to connect both ends of stator windings to power electronic converters as desired in particular configurations [2].

Mechanical swing equations can be solved either inside the model or outside using a multi-mass model. Magnetic saturation is also incorporated into this model [19]. The machine accepts d- and q-axis data both in the form of reactances and time constants. Another menu receives machine zero sequence reactances and resistances in pu.

TABLE I shows the approximate execution time (on a IBM Power 8 processor [18]) for the machine with different number of phases.

TABLE I
EXECUTION TIME VS NUMBER OF PHASES

Number of Phase	3	6	9	12
Execution Time (ns)	446	690	997	1330

IV. VALIDATION OF THE MODEL AND TIME-DOMAIN SIMULATION RESULTS

This section provides validations for the multi-star synchronous machine model presented in this paper. The focus of this section is to provide validations for the capability of the proposed model in accurately solving the differential equations of a symmetrical multi-phase synchronous machine stated in (2) - (5). To validate the performance of the proposed model in transient conditions, a small off-line stand-alone electromagnetic transient program including a stand-alone multi-star synchronous machine model is developed. The differential equations of the multi-star synchronous machine are solved with the more accurate *phase domain* approach [20] with the simulation time step of 1.0 μs.

The data for the synchronous machine under the test is shown in Appendix I. A larger salient-pole synchronous machine such as the one used here provides more distinct transient and sub-transient time constants, and consequently a more thorough validation. To check the validity of the model for a synchronous machine with multiple stars, a 2-star and a 3-star synchronous machine are modeled. Transient behavior of the model is studied under both symmetrical and asymmetrical faults.

A. Symmetrical Fault on a 2-Star (6-Phase) Synchronous Machine

In this section, the proposed multi-star synchronous machine model is configured to be a 2-star synchronous machine with 3 phases per star. During the simulation, while the rotor speed is set to synchronous, the machine is operating in open-circuit and its field voltage is adjusted such that the terminal voltage of 1 pu is achieved (1 normal field voltage).

After reaching steady state conditions, a solid 6-phase short-circuit is applied to the terminals of the machine. The fault is applied at the time that phase A1 voltage crosses zero. Variations of the field current and the stator phase A1 current of the machine for the first 3.0 seconds of the short circuit is shown in Figures 4a and 4b respectively. In each figure, there are two curves, one corresponding to the real-time model labeled as "Proposed Model", and the other corresponding to the off-line phase domain solution labeled as "Off-Line Solution".

As shown in Fig 4, the two curves are indistinguishable, establishing the fact that the proposed model is equivalent to the off-line phase-domain machine model. Consequently, the integrity of transformations used in this paper is validated.

B. Asymmetrical Fault on a 2-Star (6-Phase) Synchronous Machine

In this section, again the 2-star (6-phase) machine is used. The above experiment in Section IV-A is repeated with a solid A *phase-phase* short-circuit. Note that applying a phase-phase fault excites the zero sequence circuits in addition to the d- and q-axes circuits.

In steady-state, a solid phase-phase short-circuit is applied to each terminal A of the two stars at the zero-crossing of the phase A1 voltage. Other phases were left open. Variations of the field current and the stator phase A1 current of the machine for the first 3.0 seconds of the short circuit is shown in Figures 5a and 5b respectively. As can be seen again, the results are matching.

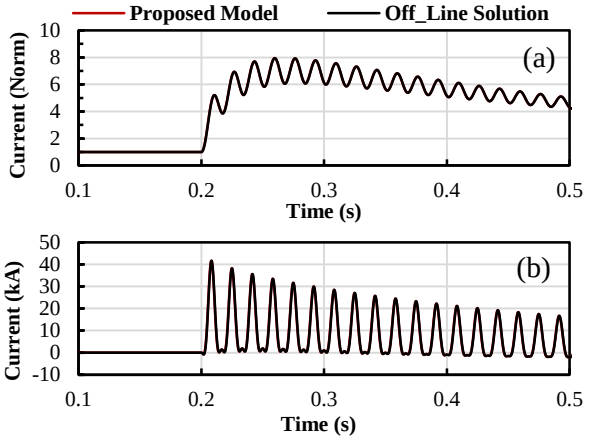

Fig. 4. 6-phase fault on a 2-star (6-phase) synchronous machine. (a) Field winding current. (b) Stator phase A1 current. Results overlap.

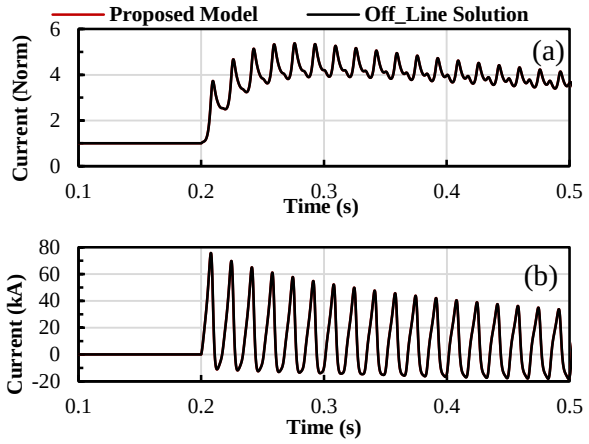

Fig. 5. Phase-phase fault on a 2-star (6-phase) synchronous machine. (a) Field winding current. (b) Stator phase A1 current. Results overlap.

A. Asymmetrical Fault on a 3-Star (9-Phase) Synchronous Machine

The experiment is repeated with a 3-star synchronous machine with 3 phases per star. In steady-state, a solid phase-neutral short-circuit is applied to terminal A1 of the machine at the zero-crossing of the phase A1 voltage. Other phases were left open. The simulation results for the field current and the stator phase A1 current are shown in Figures 6a and 6b respectively. As can be seen again, the results are identical to the off-line phase domain solution.

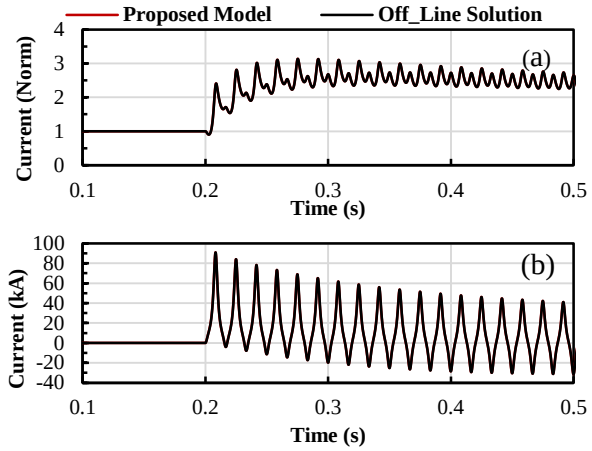

Fig. 6. Single-phase fault on a 3-star (9-phase) synchronous machine. (a) Field winding current. (b) Stator phase A1 current. Results overlap.

V. An Application Example of the Multi-Star Synchronous Machine Model in Electric Ship Systems

In this section, a typical electric network of a marine vessel [21] consisting of a dual star generator, rectifiers, a DC bus, battery storage, hotel load and propulsion system is simulated in real-time. The circuit diagram is depicted in Fig. 7.

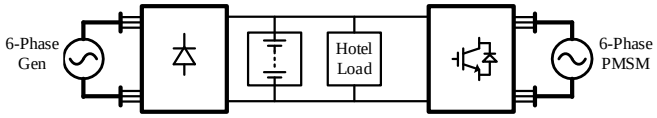

Fig. 7. The diagram for the simulated electric ship circuit.

The generator is a 4.0 *MVA*, 1.6 *kV*, 50 *Hz*, dual-star 6-phase synchronous machine. Its voltage is rectified using two 3-phase diode rectifiers. The DC bus voltage is maintained at 1.8 *kV* in normal operation of the system by means of the generator excitation system. The battery system and a hotel load of 75 *kW* is connected to the DC bus. The propulsion system consists of two VSC-based converters driving a permanent magnet synchronous motor and a mechanical load. The motor is a 1.6 *MW*, 0.69 *kV*, 6-phase dual-star PMSM. The torque and ultimately the speed of the motor is controlled using the dq decoupling method. The q- component of the stator current is used to control the torque, while the d-component is used to control the reactive power absorbed by the motor. The details of control strategy are out of the scope of this paper and are not described here. The control principles are adapted from the control techniques used in a typical PMSM wind turbine generator [22]. The circuit, including multi-star machines, power electronic converters and local generation of gating signals is simulated in real-time with the time step of 3 µs.

A. Switched Resistance Representation of Power Electronic Converters

Earlier generations of real-time power electronic converters for high frequency switching are usually emulated by using an L/C associated discrete (L/C-ADC) in a fixed time-step simulation [23]. This method has the advantage of maintaining constant Dommel equivalent admittance for ON and OFF state of the switches. However, it causes unrealistically high virtual losses, especially during high PWM frequencies. The method also causes fictitious current oscillations during switching due to the presence of inductive and capacitive components

Recently, resistive switching power electronic models have been used for real-time simulation [24]. One of the requirements for such detailed simulation of power electronic converters is the capability to decompose the admittance matrix of the network in every time-step. Fortunately, such capacities have recently become feasible with the introduction of higher performing processor cores [18].

Another important performance enhancement of the new converter models is their capability for reliable prediction of switching states in each time-step. This algorithm allows the simulation results to be free of erroneous spikes, even in the absence of iteration [24].

B. Performance of the Multi-Star Generator in Steady-State

As mentioned earlier, the generator supplies the DC bus voltages through diode rectifiers. In steady state, the positive and negative rails of the DC bus are charged to +/-0.9 kV, maintaining the total voltage of 1.8 kV. The battery system and the hotel load is also connected to the DC bus. The generator is continuously charging the battery and simultaneously provides power for the propulsion system. With the speed of motor at 1.0 pu and the battery charged to 75%, the generator produces around 2.2 MW of power. The steady state voltages, currents and electric torque of the generator are shown in Fig. 8. As expected, generator currents represent the dual star arrangement of the windings and electric torque contains the 12th harmonic.

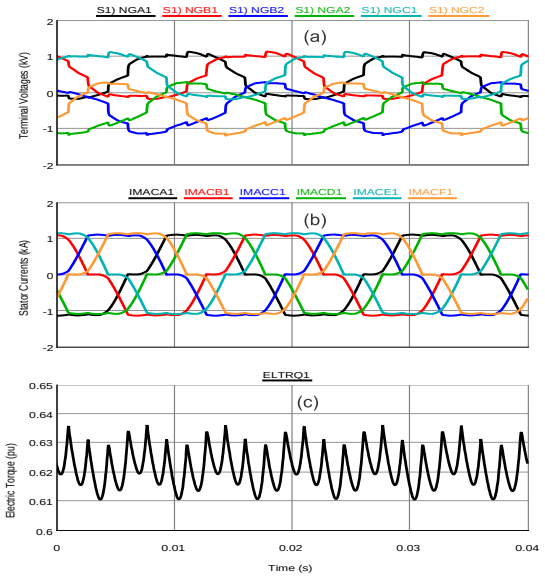

Fig. 8. Dual star generator steady state signals.

C. Performance of the Motor Drive System during the Loss of a Converter Leg

As mentioned earlier, the PMSM is supplied through two 3-phase converters based on PWM switching. One of the advantages of multiphase machines is their capacity to operate even with the loss of one or more phases. Here in steady state, the speed of machine has reached 1.0 pu and it absorbs 1.5 MWs. The voltages from phase A of converters 1 and 2 are depicted in Fig. 9(a).

This Figure also shows the firing pulses to each of the converter switches. The gating signals to phase A of converter 1 are suddenly blocked, and the variation of voltages are

shown in Fig. 9(a). Note that, even with the loss of a converter leg, the motor maintains its speed.

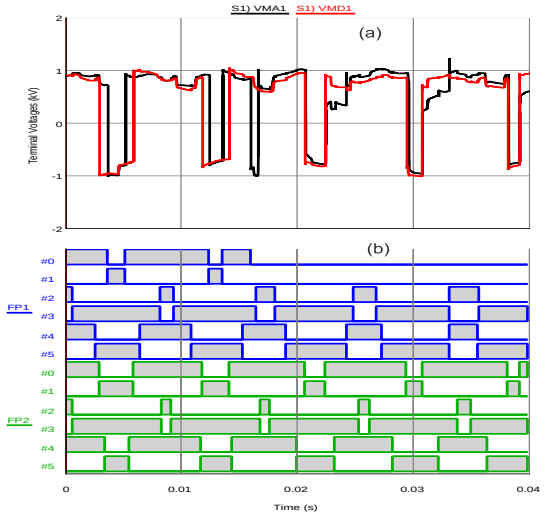

Fig. 9. PMSM terminal voltages (A1 and A2) and converter gating signals

VI. Appendix I

TABLE II
PARAMETERS OF THE SYNCHRONOUS MACHINE

Per-Unit Base	**Value**
Line-neutral rated voltage	7.97 kV
Rated MVA	100 MVA
Rated Frequency	60 Hz
D- and Q-axes Parameters	**Value (pu)**
Stator Leakage Reactance	0.13
D-axis Unsaturated Magnetizing Reactance	1.66
Field Winding Leakage Reactance	0.0618
D-axis Damper Leakage Reactance	0.00546
Q-axis Magnetizing Reactance	1.58
Q-axis Damper Leakage Reactance	0.3293
Stator Resistance	0.002
Field Resistance	0.001407
D-axis Damper Resistance	0.00407
Q-axis Damper Resistance	0.01415
Zero Sequence Parameters	**Value (pu)**
Homo-polar Zero Sequence Reactance	0.13
Homo-polar Zero Sequence Resistance	0.002
Third Harmonic Zero Sequence Reactance	0.0325
Third Harmonic Zero Sequence Resistance	0.002
Fifth Harmonic Zero Sequence Reactance	0.0195
Fifth Harmonic Zero Sequence Resistance	0.002

VII. Conclusions and Contributions

Analysis of multi-star synchronous machines is presented using a generalized method of vector space decomposition (VSD).

A detailed and flexible transient multi-star synchronous machine model was developed and validated for real-time digital simulation. The method is applicable to off-line electromagnetic transient programs as well. A typical power system circuit of a marine vessel is simulated using the introduced model.

VIII. References

[1] Toliyat, H. A, "Analysis and Simulation of Five-Phase Synchronous Reluctance Machines Including Third Harmonic of Airgap MMF", *IEEE Trans. On Industry Application*, vol. 34, no.2, pp. 332-339, April 1998.

[2] L. Parsa, "On advantages of multi-phase machines", Industrial Electronics Society, 2005. IECON 2005 , Raleigh, Nov *2005*.

[3] E. Levi, "Multiphase Electric Machines for Variable-Speed Applications," *IEEE Trans. on Industrial Electronics*, Vol. 55 (5), May 2008, pp. 1893-1909.

[4] E.A. Klingshirn, "High Phase Order Induction Motors - Part I-Description and Theoretical Considerations", *IEEE Trans. On Power Apparatus and Systems*, vol. PAS-102, no.1, pp. 47-53, Jan. 1983.

[5] R. H. Park, "Two reaction theory of synchronous machines, Part 1," *AIEE Transactions*, vol. 48, pp. 716-730, 1929.

[6] R. H. Park, "Two reaction theory of synchronous machines, Part 2," *AIEE Transactions*, vol. 52, p 352, 1933.

[7] A. Tessarolo, "Modeling and analysis of multiphase electric machines for high-power applications," Ph.D. thesis, University of Trieste, 2011.

[8] A. Tessarolo, "On the modeling of poly-phase electric machines through vector-space decomposition: theoretical considerations," IEEE Int. Conf. on Power Engineering, Energy and Electrical Drives POWERENG, Lisbon, Portugal, pp. 519 - 523, 2009.

[9] A. A. Rockhill and T. A. Lipo, "A generalized transformation methodology for polyphase electric machines and networks," IEEE Int. Electric Machines & Drives Conf. IEMDC, Coeur d'Alene, ID, USA, pp. 27 - 34, 2015.

[10] I. Zoric, M. Jones and E. Levi, "Vector Space Decomposition Algorithm for Asymmetrical Multiphase Machines," International Symposium on Power Electronics (Ee), Novi Sad, Serbia, 2017.

[11] H. W. Dommel, "Digital computer solution of electromagnetic transients in single and multiphase networks" ,IEEE Trans. Power Apparatus and Systems, vol.PAS-88, No.4, pp. 388-399, Apr. 1969.

[12] R. F. Schiferl, C. M. Ong, "Six Phase Synchronous Machine with AC and DC Stator Connections, Part I: Equivalent Circuit Representation and Steady-State Analysis", *IEEE Trans. On Power Apparatus and Systems*, vol. PAS-102, no.8, pp. 2685 - 2693, Aug. 1983.

[13] M.R. Aghaebrahimi, and R.W. Menzies, "A transient model for the dual wound synchronous machine", International Power System Transient (CCECE 1997), St John's, May, 1997.

[14] Charles L. Fortescue, "Method of Symmetrical Co-Ordinates Applied to the Solution of Polyphase Networks," *AIEE Transactions*, vol. 37, part II, pp. 1027–1140, 1918.

[15] Y. H. Ku, "Transient Analysis of AC Machinery," *AIEE Transactions*, vol. 48, p. 707, 1929.

[16] S. A. Nasar, Electromechanical energy conversion in nm-winding double cylindrical structures in presence of space harmonics", IEEE Transactions on Power App. And Systems, Vol. PAS-87, No.4, April 1968, pp. 1099-1106.

[17] P.L. Alger, Induction Machines Their Behavior and Uses, New York, Gordon and Breach, Science Publishes, 1970.

[18] *Quick Reference Guide for Power8® Processor-based Servers*, IBM® Power Systems™, 2017.

[19] T.L. Maguire, "An Efficient Saturation Algorithm for Real Time Synchronous Machine Models using Flux Linkages as State Variables," Electrimacs 2002, Montreal, Canada, June 2002. *IEEE Trans. Power Apparatus and Systems*, vol. PAS-103, no. 9, pp. 2446-2451, Sept. 1984.

[20] A. B. Dehkordi, P. Neti, A.M Gole, and T.L. Maguire, "Development and Validation of a Comprehensive Synchronous Machine Model for a Real-Time Environment", *IEEE Trans. On Energy Conversion*, vol. 25, no.1, pp. 34-48, Mar 2010.

[21] M. R. Patel, Shipboard Propulsion, Power Electronics, and Ocean Energy, New York, CRC Press, 2012.

[22] N.P.W. Strachan, D. Jovcic, "Stability of a Variable−Speed Permanent Magnet Wind Generator with Weak AC Grids", *IEEE TPD* Vol.25, No.4 Oct. 2010, pp. 2779−2788.

[23] T. Maguire and J. Giesbrecht, "Small timestep (<2 μs) VSC Model for the Real Time Digital Simulator", International Conference on Power System Transients (IPST´05) in Montreal, Canada, June 19-23, 2005, paper No. IPST05-168.

[24] T. Maguire, S. Elimban, E. Tara and Yi Zhang "Predicting Switch ON/OFF Statuses in Real Time Electromagnetic Transients Simulations with Voltage Source Converters", The 2nd IEEE Conference on Energy Internet and Energy System Integration (EI2), Beijing, China, Oct. 20-22, 2018.